

RESEARCH ARTICLE

Staged anticonvulsant screening for chronic epilepsy

Yevgeny Berdichevsky^{1,a}, Yero Saponjian^{2,3,a}, Kyung-II Park^{4,a}, Bonnie Roach⁵, Wendy Pouliot⁵, Kimberly Lu⁶, Waldemar Swiercz^{2,3}, F. Edward Dudek⁵ & Kevin J. Staley^{2,3}¹Department of Electrical and Computer Engineering and Bioengineering Program, Lehigh University, Bethlehem, Pennsylvania 18015²Department of Neurology, Massachusetts General Hospital, Boston, Massachusetts 02129³Harvard Medical School, Boston, Massachusetts 02129⁴Department of Neurology, Seoul National University Hospital Healthcare System Gangnam Center, Seoul, South Korea 06236⁵Department of Neurosurgery, University of Utah School of Medicine, Salt Lake City, Utah 84108⁶Boston University School of Medicine, Boston, Massachusetts 02119

Correspondence

Kevin J. Staley, Department of Neurology, Massachusetts General Hospital, Boston, MA 02129. Tel: 617 643 0363; Fax: 617 643 0141; E-mail: Staley.Kevin@mgh.harvard.edu

Funding Information

This work was supported by NINDS grants NS072258, NS086364, and NS077908.

Received: 1 September 2016; Revised: 15 September 2016; Accepted: 15 September 2016

Annals of Clinical and Translational Neurology 2016; 3(12): 908–923

doi: 10.1002/acn3.364

^aThese authors contributed equally to this work.

Abstract

Objective: Current anticonvulsant screening programs are based on seizures evoked in normal animals. One-third of epileptic patients do not respond to the anticonvulsants discovered with these models. We evaluated a tiered program based on chronic epilepsy and spontaneous seizures, with compounds advancing from high-throughput in vitro models to low-throughput in vivo models. **Methods:** Epileptogenesis in organotypic hippocampal slice cultures was quantified by lactate production and lactate dehydrogenase release into culture media as rapid assays for seizure-like activity and cell death, respectively. Compounds that reduced these biochemical measures were retested with in vitro electrophysiological confirmation (i.e., second stage). The third stage involved crossover testing in the kainate model of chronic epilepsy, with blinded analysis of spontaneous seizures after continuous electrographic recordings. **Results:** We screened 407 compound-concentration combinations. The cyclooxygenase inhibitor, celecoxib, had no effect on seizures evoked in normal brain tissue but demonstrated robust antiseizure activity in all tested models of chronic epilepsy. **Interpretation:** The use of organotypic hippocampal cultures, where epileptogenesis occurs on a compressed time scale, and where seizure-like activity and seizure-induced cell death can be easily quantified with biomarker assays, allowed us to circumvent the throughput limitations of in vivo chronic epilepsy models. Ability to rapidly screen compounds in a chronic model of epilepsy allowed us to find an anticonvulsant that would be missed by screening in acute models.

Introduction

In the absence of sufficiently detailed insights into the pathophysiology of epilepsy,¹ development of anticonvulsant therapies has relied on empirical drug screening efforts. Decades of screening and subsequent drug development have produced many new anticonvulsants, yet, epilepsy remains medically intractable in one-third of patients.² Recently, it has been proposed that this lack of progress is a consequence of the method by which compounds are screened.^{3,4} To date, initial screening is based on acute application of convulsant conditions to normal brain tissue,^{2,4} but this produces patterns of epileptic activity that are substantially different from spontaneous

epileptiform activity in chronically epileptic brain tissue.⁵ Thus, we considered the hypothesis that screening for anticonvulsants in chronically epileptic tissue would uncover agents that may be uniquely effective in medically intractable epilepsy.⁶

Unfortunately, most epileptiform activity in chronically epileptic brain is comprised of brief interictal electrographic spikes. While not benign,⁷ spikes are not the target of anticonvulsants.⁸ Actual seizure activity in experimental epilepsy is rare, unpredictable, and develops slowly after an inciting brain injury.⁹ Morbidity and mortality are significant once seizure frequencies are sufficiently high for screening studies.¹⁰ At all seizure frequencies, clustering of seizures substantially increases

the sampling required to discern anticonvulsant effects.¹¹ Thus, *in vivo* models of chronic seizures have not been practical for drug screening. Accordingly, we developed a staged screening program in which initial evaluations are based on spontaneous seizures in a chronically epileptic *in vitro* preparation in which these practical shortcomings are obviated.

Organotypic hippocampal slice cultures¹² preserve the key circuitry of the *in vivo* hippocampus.¹³ However, brain slice preparation involves massive traumatic axotomy at the cut surfaces, so that the slice can be considered a model of severe traumatic shear injury and an *in vitro* extension of the undercut cortical model of posttraumatic epilepsy.¹⁴ As a consequence of the deafferentation, robust sprouting takes place,^{15,16} so that connectivity between pyramidal cells increases from 3% in acute slices to 30% in organotypic slices.^{17,18} In light of this abundant reciprocal excitation, it is not surprising that organotypic slice cultures are hyperexcitable¹⁹ and even spontaneously epileptic^{20,21} (see Heinemann and Staley²² for review). We have characterized epileptogenesis in this preparation.^{23,24} Increases in extracellular lactate accompanied seizures in human hippocampus,^{25,26} and we found that lactate production was correlated with seizure-like activity in organotypic cultures. Lactate dehydrogenase (LDH) is released into culture medium after plasma membrane loses its integrity,^{27–29} and its concentration is correlated with cell death in cultures. We then demonstrated that this preparation and lactate and LDH assays can be used to evaluate anticonvulsant efficacy, using phenytoin and manipulation of mTOR pathway as examples.^{30,31} We now show the utility of this *in vitro* model of chronic epilepsy as a first, blinded, moderate throughput stage for drug screening. Repeat biochemical as well as electrophysiological confirmation *in vitro* comprised the second stage of screening. The final stage was comprised of double blind, crossover controlled, *in vivo* testing in the kainate model of severe chronic epilepsy^{9,32} with seizure quantification by continuous electrographic monitoring.³³

Materials and Methods

Organotypic hippocampal cultures

Hippocampal slices of 350 μm thickness were dissected from postnatal day 7–8 Sprague–Dawley male rat pups (Fig. 1A). Slices were placed onto poly-D-lysine (PDL)-coated 6-well tissue culture plates (Fig. 1B and C). Culture medium consisted of Neurobasal-A/B27 supplemented with 0.5 mmol/L GlutaMAX and 30 $\mu\text{g}/\text{mL}$ gentamicin (Life Technologies). Slices were maintained at 37°C in a humidified atmosphere that contained 5% CO₂. After attachment, culture plates were placed on a rocking

platform (Fig. 1D and E). All of the procedures conformed to the NIH guidelines (i.e., as described in The Guide for Care and Use of Laboratory Animals) and were approved by the Massachusetts General Hospital Subcommittee on Research Animal Care.

Compound application and assays

We organized cultures into four experimental groups of three slices each, all from the same animal (Fig. 1C).

Compounds were applied starting from day *in vitro* (DIV) 3, and reapplied with every biweekly medium change (Fig. 1I), except wash-out experiments where compound application stopped on indicated DIV. To blind the experimenter, compounds and vehicle controls were labeled with randomly assigned numbers. Maps of compound/vehicle numbers and corresponding experiments were maintained by a different investigator. Culture supernatant (spent culture medium) was collected and relative concentrations of markers of seizure-like activity and ictal neuronal death, lactate, and LDH, were measured using commercially available kits (Biovision, Milpitas, CA).

Morphology scoring

The natural progression of slice morphology over first 24 days *in vitro* is shown in the first column of Figure 1F. We noticed that some drugs significantly altered slice morphology, and that these changes correlated with the number of surviving neurons in the slice. We therefore developed a scoring metric for morphology that was used together with LDH measurements to screen drugs and compounds for toxicity. Slices that appeared lighter or same as controls were assigned a score of 0, slices that were smaller or darker than controls were assigned a score of 1, slices with significantly changed shape or with neuronal layers that were no longer distinguishable were assigned a score of 2, and slices which disintegrated or detached from substrate were assigned a score of 3 (Fig. 1F).

Toxicity screening

We found that some drugs were toxic to organotypic hippocampal cultures at applied concentrations, as measured by increased LDH on DIV 6/7 or by morphology scoring. While morphology and LDH were well correlated ($r^2 = 0.6$, $P < 0.001$, $n = 407$ drug-concentration pairs), several compounds or drugs increased LDH without a corresponding change in morphology, while others changed the morphology without a corresponding change in LDH (Fig. 2A). This may be due to different modes of cell death.²⁷ We therefore adopted the following criteria for establishing toxicity of a given drug-concentration

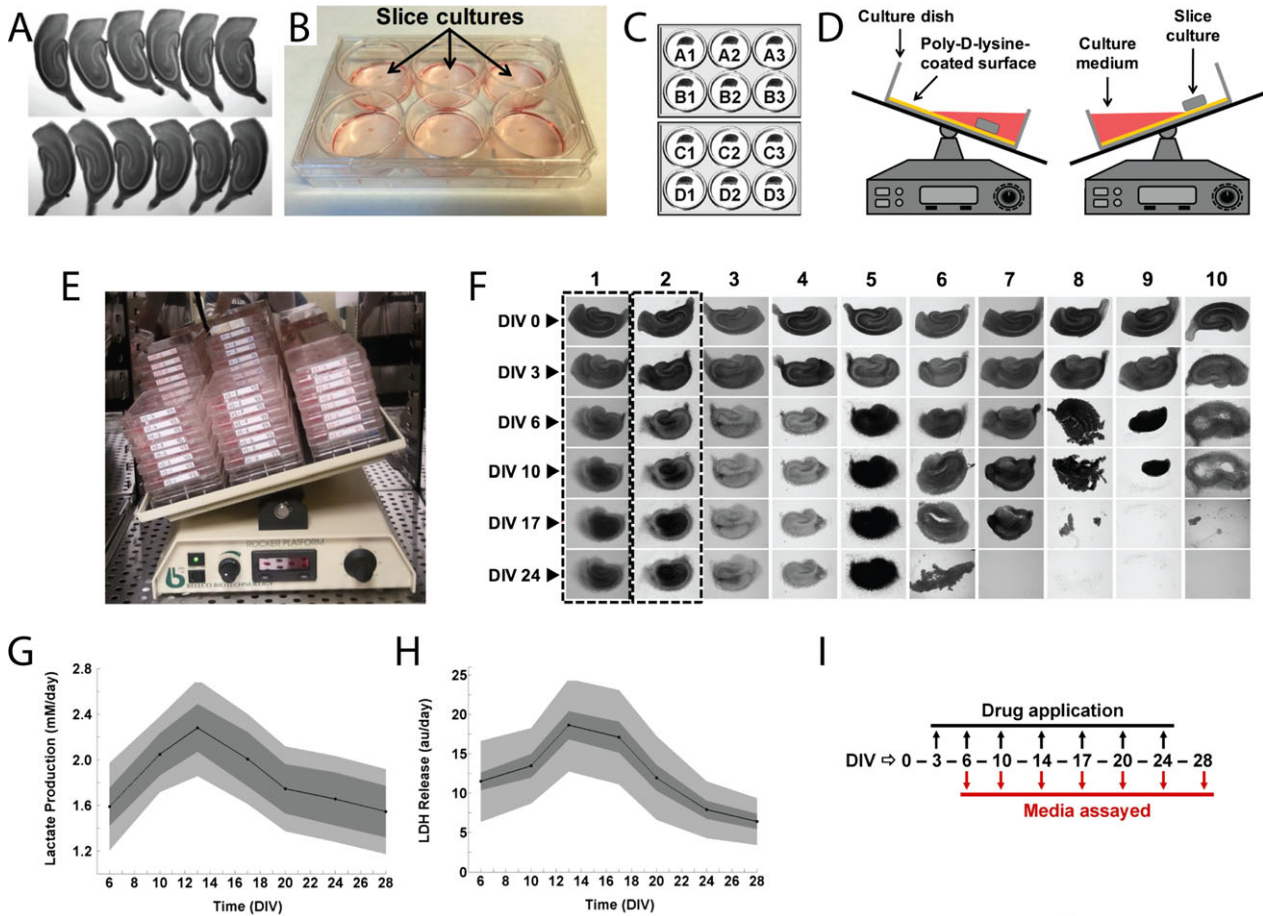


Figure 1. Screen design. (A) Twelve hippocampal slices derived from the same rat pup, imaged on day in vitro (DIV) 0 immediately after dissection. (B) Photograph of slice cultures in a poly-D-lysine-coated 6-well tissue culture plate with culture medium. (C) Twelve slices were cultured in four sets of triplicates, allowing for screening of four conditions per experiment. One of the four conditions tested per experiment was always a control (vehicle). (D) A single well of a 6-well plate with a slice culture is shown in cross-section on a rocking platform. Slice was offset from the center of the well allowing it to be submerged in culture medium and aerated in a continuously alternating manner during rocking. (E) Slices were cultured in 6-well plates on a rocking platform in a humidified chamber with 5% CO₂ at 37°C. (F) Morphological progression of a control organotypic hippocampal slice culture over 24 days in vitro is shown in column 1. The toxic effects of various compounds (first application on DIV 3) on organotypic hippocampal slice cultures (columns 3–10) in comparison with a compound with a nontoxic effect (column 2) are also shown. (G) Lactate production and (H) Lactate dehydrogenase (LDH) release measured in spent culture media from control organotypic hippocampal slice cultures (*n* = 318 slices) as biomarkers of seizure-like activity and ictal neuronal death, respectively. The lighter gray areas represent the overall population variation, whereas the darker gray areas represent the intertriplicate variation. Data are expressed as mean ± SD. (I) Chronic application experiments were carried out for 28 days in vitro with compounds added to culture media starting on DIV 3. Every 3–4 days, spent culture medium was collected and fresh culture medium with appropriate drug(s) was added to slice cultures. Collected spent culture medium was assayed for biomarkers of seizure activity and ictal neuronal death.

pair: (1) morphology score >0, or (2) LDH on DIV 6/7 that was significantly higher than control. If either criterion was satisfied by a drug-concentration pair, this pair was deemed toxic and excluded from further analysis.

Data analysis and statistics

The strictly standardized mean difference (SSMD) metric was used to identify hits in the compound screen. SSMD was calculated according to the following formula:

$$SSMD_i = \frac{\bar{X}_i - \bar{X}_N}{\sqrt{s_i^2 + s_N^2}}$$
 where \bar{X}_i is the mean of integrated lactate or LDH values for drug *i*, \bar{X}_N is the mean of integrated lactate or LDH for matched control, and S_i^2 and S_N^2 are drug and control variances, respectively. SSMD captures information about both the size of the effect (difference between drug and control means) and significance of the result, similar to Cohen's D.³⁴ We used the following criteria: |SSMD| > 3 (very strong effect), 3 > |SSMD| > 2 (strong effect), 2 > |SSMD| > 1.645

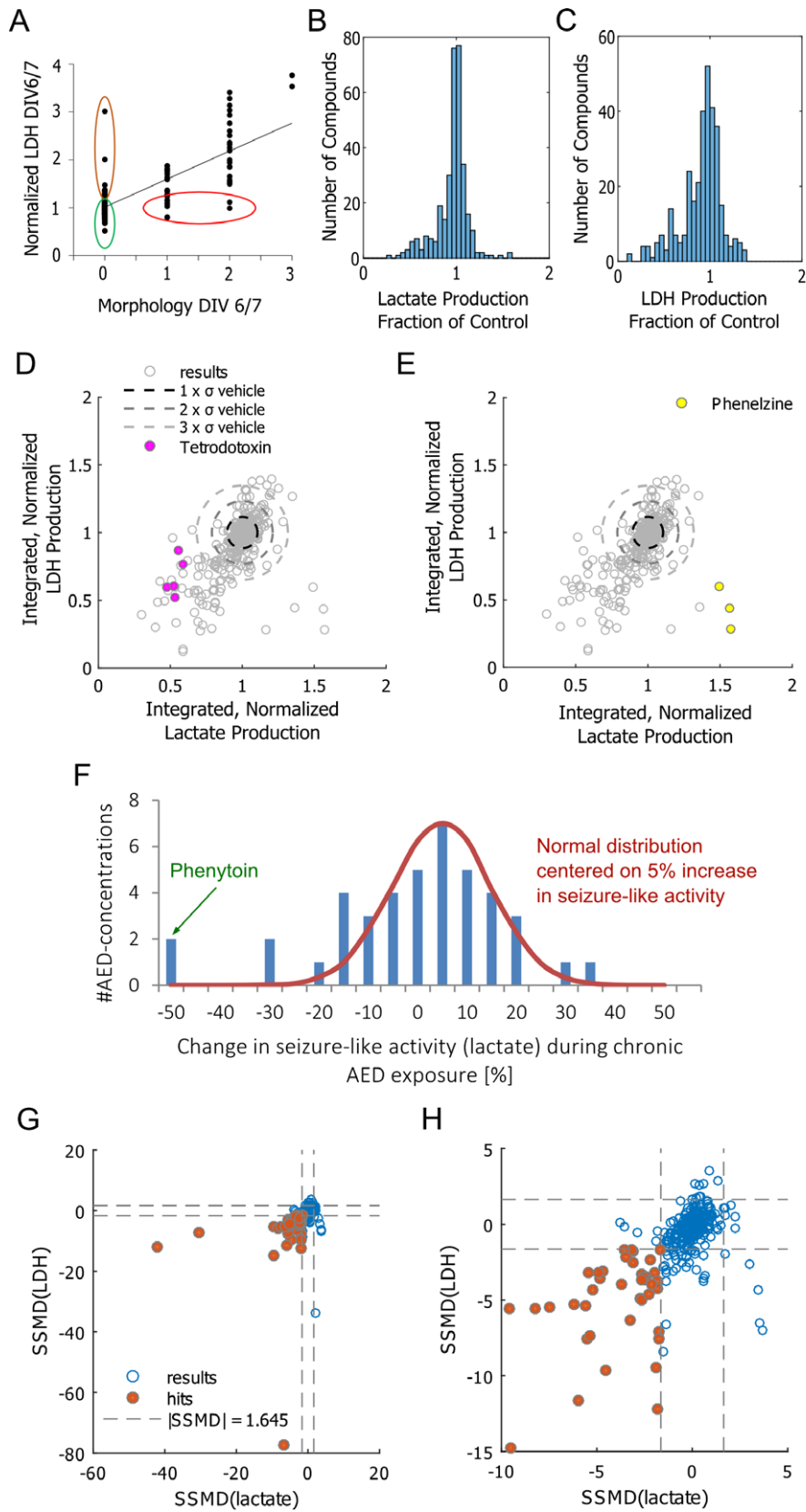


Figure 2. Drug effects. (A) Lactate dehydrogenase (LDH) values and morphology scores on day in vitro (DIV) 6/7 were well correlated ($R^2 = 0.6019$, $P < 0.001$), suggesting that cell death led both to increased LDH release and changed culture morphology. However, in a few cases, applied compounds caused a significantly higher LDH release without accompanying change in morphology (brown outline). In other cases, differences in morphology were observed without a significant difference in LDH release (red outline). These compounds were also excluded from analysis. Compounds that were included in analysis are outlined in green. (B, C) Histograms of frequency of screened nontoxic compounds as fraction of controls for lactate production (B) and LDH release (C) (328 drug-concentration pairs; $n = 3$ slices per pair). (D) Integrated lactate production (DIV 10–17), normalized to controls from the same pup versus integrated LDH production (DIV 1017), normalized to controls. σ = standard deviation of integrated lactate (horizontal axis) and LDH (vertical axis) of vehicle-treated controls. Data are plotted for 328 drug-concentration pairs. Effects of tetrodotoxin (D) and phenelzine (E) are highlighted for separate experiments ($n = 3$ each experiment) that were performed over 2–3 years to demonstrate reproducibility of the screen. (F) Histogram of effects of standard AEDs on seizure-like activity (measured by lactate production) in organotypic hippocampal cultures. Normal distribution is included in the same plot for comparison. (G) Strictly standardized mean difference (SSMD) values of lactate and LDH production of drug-treated cultures versus vehicle-treated controls, evaluated between DIV 10–17. Significant results (SSMD < -1.645 for both lactate and LDH) are highlighted with brown color. (H) Same plot as (G), shown in more detail.

(fairly strong effect), $1.645 > |\text{SSMD}| > 1$ (moderate effect), $1 > |\text{SSMD}| > 0$ (weak effect).³⁵ P values for screen hits were calculated using Student's t -test.

Acute recordings

Extracellular field potentials were recorded in the CA1 and/or CA3 pyramidal cell layer of intact hippocampi³⁶ and organotypic hippocampal slices in a conventional submerged chamber using tungsten-coated microelectrodes and ISO-DAM8A amplifier (World Precision Instruments). Oxygenated (95% O₂ and 5% CO₂) artificial cerebrospinal fluid containing 126 mmol/L NaCl, 3.5 mmol/L KCl, 2 mmol/L CaCl₂, 1.3 mmol/L MgCl₂, 25 mmol/L NaHCO₃, 1.2 mmol/L NaH₂PO₄, and 11 mmol/L glucose (pH 7.4), was continuously perfused at $33 \pm 0.5^\circ\text{C}$. Flow rate was 2.5 mL/min. Before the actual recording, slices were allowed to stabilize in the recording chamber for 30–60 min. Electrical signals were digitized using an analog-to-digital converter (DigiData 1322A, Axon Instruments). pCLAMP 8.2 (Axon Instruments) and SigmaPlot 11.0 (Systat Software) programs were used for data acquisition and analysis. Recordings were sampled at 10 KHz and filtered from 1 Hz to 2 kHz. Ictal-like epileptiform discharges were defined as hyper-synchronous large amplitude ($\times 3$ baseline) and high-frequency population spikes followed by sustained ictal-tonic and intermittent ictal-clonic after discharges, with the duration of the population spike and after-discharge complex lasting more than 5–10 sec. Power spectrum analysis was performed from the electrical signals after applying a Hamming window function.

In vivo experiments

Kainate treatment and induction of status epilepticus

A description of the methods for and characteristics of the repeated, low-dose kainate model have been published in detail elsewhere.^{9,10,37} Briefly, convulsive status epilepticus

was induced in adult male Sprague–Dawley rats (180–200 g) with repeated (i.e., approximately every 30 min), low-dose (7.5 mg/kg), intraperitoneal (IP) injections of kainic acid (Tocris Bioscience, Bristol, UK). During and after the kainate treatment, all rats were maintained in a climate-controlled vivarium. All of the procedures conformed to the NIH guidelines (i.e., as described in The Guide for Care and Use of Laboratory Animals) and were approved by the University of Utah Animal Care and Use Committee (IACUC).

Surgical implantation of recording electrodes

Rats with kainate-induced epilepsy were implanted with cortical electroencephalogram (EEG) electrodes. The head was held in a stereotaxic device, and the surgical site was clipped and washed with Betadine scrub and solution. The rat was anesthetized with 2% isoflurane and pretreated with 0.8 mL subcutaneous atropine (0.54 mg/kg) and 0.2 mL subcutaneous dexamethasone (4 mg/mL). After the incision and retraction of the skin, the dura was removed and six small holes were drilled through the skull, for implantation of support screws and electrodes. A bipolar stainless-steel recording electrode pedestal was lowered onto the cortex of the right hemisphere (4.0 mm lateral, 8.0 mm caudal), and a ground electrode was placed on the cortex of the left hemisphere (2.0 mm lateral, 3.5 mm rostral). Dental acrylic fastened the electrode pedestal into place and covered and sealed the exposed skull surfaces. The incision was closed with 4–0 Dermalon sutures to the level of the dental cement covering the skull. Animals were then administered subcutaneous treatments of 3.0 mL lactated Ringer's, 0.1 mL marcaine (0.5%), 0.1 mL buprenorphine (0.3 mg/mL), and 0.2 mL penicillin (300,000 IU).

Chronic in vivo recordings

Rats with kainate-induced epilepsy and implanted electrodes were placed in custom-built Plexiglass recording

chambers equipped with swivel commutators, and connected to spring-covered cables (Plastics One, Roanoke, VA) to their skull caps. Electrographic signals were amplified with EEG100C amplifiers (high-pass at 1 Hz; low-pass at 100 Hz; notch filter at 60 Hz), digitized at 500 Hz with an MP150 digital-analog converter, and acquired with AcqKnowledge software (BioPac Systems Inc.; Santa Barbara, California). Electrographic recordings were obtained continuously during vehicle and drug treatments. Data were stored on hard-drives for offline analysis using AcqKnowledge software.

Repeated-measures, crossover protocol for drug testing

Long-term, continuous recording sessions were used to assess the effect of Celecoxib-containing food versus control food on spontaneous recurrent electrographic seizures. A repeated-measure, crossover protocol was used with 100 mg/kg/day Celecoxib in custom-made food (Bio-serv).³⁸ The 100 mg/kg/day dose of Celecoxib would be equivalent to five injections of 20 mg/kg/day.³⁹ Each trial involved eight treatments of Celecoxib and eight vehicle treatments administered on alternate days with two recovery days between the treatment days. The rationale for the repeated-measure, crossover design was the high degree of statistical power inherent in this approach. For example, for $\alpha = 0.05$, eight animals and six drug-versus-vehicle crossovers (i.e., a total of 48 drug-versus-vehicle tests per trial³⁸) yields a power of 0.9.

Blinded seizure detection

EEG acquisition and analysis were performed at separate sites by different investigators. DClamp (sourceforge.net) was used to detect seizures using supervised algorithms.³³ Detection parameters were set to increase sensitivity to the point that seizures were rarely missed in trial detections, but false-positive detections were common. Human supervision consisted of review of all detected seizures for false-positive detections and review of raw EEG for false negatives. In total, 532 true positives, 18578 false positives, and 94 false negatives were found. To blind the supervising investigator, the EEG files and channels were renamed using random numbers, and the map to the original names was managed by an investigator not involved in the analysis.

Results

Lactate and LDH in control cultures

We followed the natural progression of lactate and LDH production by epileptic control cultures from DIV 6 to DIV

28 (Fig. 1, $n = 318$). Lactate and LDH production reached their peaks between DIV 14 and 17 (Fig. 1G and H). Decrease in lactate and LDH production at later time points is likely a consequence of seizure-induced neuron death, the peak of which occurs between DIV 14 and 17.³⁰ We therefore used the period between DIV 10 and DIV 17 (the time between the onset of spontaneous seizure-like activity and significant neuron death) to compare lactate and LDH production in vehicle-treated and drug-treated cultures. We found that variability between cultures dissected from the same animal was lower than variability between cultures dissected from different animals (Fig. 1G and H). To control for interanimal differences, all experimental assays were compared to vehicle-treated cultures from the same animal.

Compound screen results

We screened 140 compounds, including combinations of drugs (Table 1). Different concentrations were used for each drug, and a total of 407 drug-concentration pairs were screened in triplicate ($n = 3$ slices). Of these, 79 were found to be toxic (Table 2) and excluded from further analysis (Fig. 2A). We integrated the lactate and LDH production of the remaining 328 drug-concentration pairs between DIV 10 and DIV 17 ($n = 3$), and normalized it by control (vehicle-treated cultures from the same pup, $n = 3$) lactate and LDH production over the same period. Histograms of lactate and LDH production are shown in Figure 2B and C, and a scatter plot of lactate versus LDH is shown in Figure 2D. Values that are lower than unity indicate that a drug lowered lactate and/or LDH production to a level below that of a vehicle-treated control. Some of the low lactate and LDH values were less than the mean standard deviation lower than the mean of controls, suggesting that significant reduction of seizure-like.

We examined the long-term reproducibility of our drug screening methodology by comparing values obtained over a period of 2–3 years (Fig. 2D and E). Lactate and LDH values for tetrodotoxin and phenelzine were found to reliably cluster into the same regions of lactate versus LDH scatter plot, demonstrating the stability and reproducibility of our results.

Our screen included 42 drug-concentration pairs ($n = 3$ per drug-concentration pair) of standard antiepileptic drugs (AEDs), including acetazolamide (10 $\mu\text{mol/L}$), carbamazepine (10–70 $\mu\text{mol/L}$), diazepam (1 $\mu\text{mol/L}$), ethosuximide (10–1000 $\mu\text{mol/L}$), felbamate (0.01–1 $\mu\text{mol/L}$), gabapentin (1–50 $\mu\text{mol/L}$), levetiracetam (10–250 $\mu\text{mol/L}$), phenacemide (0.01–1 $\mu\text{mol/L}$), phenobarbital (100 $\mu\text{mol/L}$), phenytoin (100 $\mu\text{mol/L}$), pregabalin (0.01–1 $\mu\text{mol/L}$), topiramate (10–100 $\mu\text{mol/L}$), and valproate (600 $\mu\text{mol/L}$). A histogram of the effects of

Table 1. List of screened drugs and compounds.

Anticonvulsants	Cholinergic	Glutamate	Dopamine	Chloride	Antiinflammatory
Carbamazepine	Amantadine HCl	ACPD	Clomipramine	Acetazolamide	Carprofen
Diazepam	Atropine sulfate	CPPG	Dopamine HCl	Bumetanide	Celecoxib
Ethosuximide	Carbachol	DCG IV	Haloperidol	Chlorothiazide	Celecoxib +
Felbamate	Diphenhydramine	Dextromethorphan		CLP257*	Phenytoin
Gabapentin	Edrophonium	HBr	Serotonin	D4.2*	Deracoxib
Levetiracetam (keppra)	Nicotine bitartrate	dL APV	Ketanserine	Furosemide	Diclofenac
Phenacemide		Kynurenic acid	Tartrate	IS50699*	Firocoxib
Phenobarbital	Monoamine NT	L-AP4	Methysergide	Mannitol	Indomethacin
Phenobarbital +	modulators	LY341495	Zolmitriptan		Ketoprofen
Bumetanide	Amitriptyline	MPEP		Sodium	Ketorolac
Phenytoin	Amoxapine		Opioid	Bretylium Tosylate	LOXBlock-1*
Pregabalin	Atomoxetine	GABA	Nalbuphine HCl	Digoxin	Meclofenamate
Retigabine	Bupropion	Baclofen	Naloxone	Lidocaine HCl	Meloxicam
Topiramate	Clonidine	CGP55845	Tramadol	Tetrodotoxin (TTX)	Piroxicam
Valproic acid	Desipramine	Diazepam + CLP257	TG4-155*	TTX + Fluoxetine	Rofecoxib
	Doxepin	Diazepam + IS50699		TTX + Nortriptyline	Sulindac
Intracellular signaling	Duloxetine	Flurothyl	Cannabinoid		Zileuton
AG 1024	Fluoxetine	Gabazine	Rimonobant	Calcium	
Akt 1,2 kinase inhibitor	Imipramine	Taurine		Flunarizine	Antioxidant
API-2 (Triciribine)	Maprotiline		Purine	Verapamil	Acetylcysteine
DFMO	Methylphenidate HCl	Microtubule	Allopurinol		Alpha-tocopherol
Gefitinib (Iressa)	Modafinil	Colchicine	Caffeine	Potassium	GCEE*
K-252a	Nortriptyline	Vinblastine		Glipizide	
Lyothyronine	Phenelzine	Vincristine	Steroids		Growth factor
PDMP*	Phenelzine + TTX		Dexamethasone	Blinded	Neuregulin-1*
Picropodophyllotoxin	Propranolol	Antiproliferative	Estradiol	LacCer*	
Rapamycin	Reserpine	Carboplatin	Letrozole	LDN-209884(3-1)*	Cell death
Sildenafil Citrate	Selegiline	Cycloheximide	Lovastatin	LDN-212320(10-10)*	Caspase-3 inhibitor*
TGFbeta RI inhibitor*	Sertraline	Etoposide	Megestrol	LDN-72457(5-1)*	Erythropoietin
TrkB Fc chimera	Venlafaxine	AG 1478	Tamoxifen citrate		Minocycline

Drugs marked with an asterisk were obtained from collaborators, while the rest of the drugs were primarily obtained from the NINDS custom compound collection of known bioactives and FDA-approved drugs.

these drugs on lactate production, a marker of seizure-like activity in organotypics, is shown in Figure 2F. Data for individual drug-concentration pairs are included in Table S1. Phenytoin was most effective, but seizure activity recrudesces after 3 weeks of exposure, that is, the slice cultures become refractory to phenytoin.³⁰

We used the strictly standardized mean difference (SSMD) metric to make a robust determination of the significance of screen results, and to identify “hits”. SSMD takes both effect size and data variance into account, thus identifying hits that have the strongest and most statistically significant effect. We used a cutoff of SSMD <−1.645 to identify hits with a fairly strong³⁵ reduction of both lactate and LDH production (Fig. 2G, H, and Table 3). Results for all screened compounds are listed in the Table S1.

Celecoxib effect on lactate and LDH production

We found that celecoxib, an antiinflammatory drug applied at the concentration of 10 μmol/L, was a strong

inhibitor of lactate and LDH production in five separate experiments ($n = 3$ cultures, each experiment, $-9.6 < \text{SSMD}_{\text{lactate}} < -2.1$, $-9.7 \text{ SSMD}_{\text{LDH}} < -4$). Lower concentration, 1 μmol/L, was less effective, while 100 μmol/L celecoxib was toxic to organotypic cultures (Figure S1). In contrast, other antiinflammatory drugs that we have tested did not have as strong effect on lactate and LDH production (Fig. 3A).

We have previously found that anticonvulsant phenytoin is effective at suppressing ictal-like activity and seizure-induced cell death in this model of epilepsy, although the effect was temporary.³⁰ Since phenytoin and celecoxib are likely reducing seizures through different mechanisms, we examined whether celecoxib + phenytoin (C+P) combination would have a stronger and/or longer lasting effect on lactate and LDH production than celecoxib or phenytoin alone. We found that this was the case, with C+P combination reducing both lactate and LDH production beyond that of celecoxib or phenytoin alone by DIV 14 (Fig. 3C and D, lactate $P < 0.001$ versus celecoxib or phenytoin alone, LDH $P < 0.001$ versus

Table 2. List of drug-concentration pairs excluded from analysis due to early toxicity.

Drug name	Concentration	Drug name	Concentration	Drug name	Concentration
Akt 1/2 kinase inhibitor	10 $\mu\text{mol/L}$	Dextromethorphan HBr	10 $\mu\text{mol/L}$	Maprotiline	10 $\mu\text{mol/L}$
Akt 1/2 kinase inhibitor	5 $\mu\text{mol/L}$	DFMO	40 $\mu\text{mol/L}$	Megestrol acetate	10 $\mu\text{mol/L}$
Akt 1/2 kinase inhibitor	2 $\mu\text{mol/L}$	Diazepam + IS50699	1 + 10 $\mu\text{mol/L}$	Minocycline	500 $\mu\text{mol/L}$
Alpha-tocopherol	10 $\mu\text{mol/L}$	Duloxetine	10 $\mu\text{mol/L}$	Minocycline	100 $\mu\text{mol/L}$
Alpha-tocopherol	1 $\mu\text{mol/L}$	Erythropoietin	100 IU/mL	Nortriptyline	10 $\mu\text{mol/L}$
Alpha-tocopherol	0.1 $\mu\text{mol/L}$	Erythropoietin	10 IU/mL	Nortriptyline + TTX	10 $\mu\text{mol/L}$ + 1 $\mu\text{mol/L}$
Amitriptyline	10 $\mu\text{mol/L}$	Erythropoietin	1 IU/mL	Nortriptyline + TTX	1 $\mu\text{mol/L}$ + 1 $\mu\text{mol/L}$
Amoxapine	10 $\mu\text{mol/L}$	Felbamate	1 $\mu\text{mol/L}$	PDMP	50 $\mu\text{mol/L}$
API-2 (Triciribine)	10 $\mu\text{mol/L}$	Flunarizine	10 $\mu\text{mol/L}$	PDMP	25 $\mu\text{mol/L}$
API-2 (Triciribine)	5 $\mu\text{mol/L}$	Fluoxetine	10 $\mu\text{mol/L}$	Phenelzine + TTX	1 $\mu\text{mol/L}$ + 1 $\mu\text{mol/L}$
API-2 (Triciribine)	2 $\mu\text{mol/L}$	Fluoxetine	2 $\mu\text{mol/L}$	Phenelzine + TTX	0.1 $\mu\text{mol/L}$ + 1 $\mu\text{mol/L}$
API-2 (Triciribine)	1 $\mu\text{mol/L}$	Fluoxetine + TTX	10 $\mu\text{mol/L}$ + 1 $\mu\text{mol/L}$	Picropodophyllotoxin	10 $\mu\text{mol/L}$
Bupropion	10 $\mu\text{mol/L}$	Gefitinib (Iressa)	10 $\mu\text{mol/L}$	Picropodophyllotoxin	5 $\mu\text{mol/L}$
Caspase-3 inhibitor	10 $\mu\text{mol/L}$	Gefitinib (Iressa)	1 $\mu\text{mol/L}$	Picropodophyllotoxin	2 $\mu\text{mol/L}$
CGP55845	1 $\mu\text{mol/L}$	Gefitinib (Iressa)	0.1 $\mu\text{mol/L}$	Picropodophyllotoxin	1 $\mu\text{mol/L}$
CGP55845	0.1 $\mu\text{mol/L}$	IS50699	10 $\mu\text{mol/L}$	Piroxicam	10 $\mu\text{mol/L}$
CGP55845	0.01 $\mu\text{mol/L}$	IS50699	10 $\mu\text{mol/L}$	Rimonabant	10 $\mu\text{mol/L}$
Clomipramine	10 $\mu\text{mol/L}$	K-252a	1 $\mu\text{mol/L}$	Sertraline	10 $\mu\text{mol/L}$
CLP257	100 $\mu\text{mol/L}$	K-252a	0.3 $\mu\text{mol/L}$	Sertraline	2 $\mu\text{mol/L}$
CLP257	100 $\mu\text{mol/L}$	Ketanserin tartrate	1 $\mu\text{mol/L}$	Tamoxifen citrate	10 $\mu\text{mol/L}$
Colchicine	1 $\mu\text{mol/L}$	Ketanserin tartrate	0.1 $\mu\text{mol/L}$	TrkB Fc chimera	1 $\mu\text{g/mL}$
Colchicine	0.1 $\mu\text{mol/L}$	Ketanserin tartrate	0.01 $\mu\text{mol/L}$	Verapamil	100 $\mu\text{mol/L}$
Colchicine	0.1 $\mu\text{mol/L}$	LacCer	20 $\mu\text{g/mL}$	Verapamil	10 $\mu\text{mol/L}$
D4.2	10 $\mu\text{mol/L}$	LacCer	10 $\mu\text{g/mL}$	Vinblastine	0.1 $\mu\text{mol/L}$
DCG IV	10 $\mu\text{mol/L}$	LDN-212320(10-10)	10 $\mu\text{mol/L}$	Vincristine	0.1 $\mu\text{mol/L}$
DCG IV	1 $\mu\text{mol/L}$	Lidocaine HCl	10 $\mu\text{mol/L}$		
Desipramine	10 $\mu\text{mol/L}$	Lovastatin	10 $\mu\text{mol/L}$		

phenytoin alone, and $P = 0.019$ versus celecoxib alone, values from ANOVA with Bonferroni post hoc analysis, $n = 6$ each condition). Phenytoin and celecoxib were no longer effective in reducing lactate release from cultures by DIV 21, but effectiveness of C+P combination persisted until DIV 27 (C+P vs. vehicle, lactate $P < 0.001$). However, reduction in lactate release was no longer observed after wash-out of all drugs on DIV 28. We examined the effects of drug wash-out by comparing lactate values on DIV 27 (just before wash-out) and DIV 30 (3 days after wash-out). LDH values were compared between DIV 27 and DIV 31, since seizure-induced cell death peak occurs slightly after the seizure peak in this model. We found that lactate and LDH release significantly increased in celecoxib-treated cultures after celecoxib wash-out ($P < 0.001$ lactate, $P = 0.024$ LDH, paired t-test), and in C+P-treated cultures after C+P wash-out ($P < 0.001$ lactate, $P = 0.007$ LDH, paired t-test), suggesting that celecoxib has a strong anticonvulsant, but not an antiepileptic, effect.

Lack of celecoxib effect in acute seizure model

Recurrent seizures were induced in intact hippocampus preparation by perfusion of low-Mg artificial

cerebrospinal fluid (aCSF). The extracellular field potential was monitored in the CA3 area in a recording chamber perfused with low-Mg aCSF (Fig. 4A). The first appearance of seizure-like activity was observed 25.2 ± 5.0 min after exposure to low-Mg aCSF. After initial 3–10 seizures, seizure-like activities were recorded over 1 h as baseline and then 10 $\mu\text{mol/L}$ celecoxib was bath applied for another hour. Compared with baseline data before application, seizure parameters such as total number, percent change, and mean duration of seizures were not changed significantly by celecoxib (Fig. 4B) ($P = 0.86, 0.8,$ and 0.25 , respectively, $n = 5$). Interseizure interval tends to gradually decrease in this preparation over time,³⁶ but celecoxib did not revert this trend (Fig. 4B). All these results indicate that celecoxib has no effect on acute epileptiform activity induced by low-Mg in intact hippocampi from naïve animals.

Electrographic effects of celecoxib in chronic seizure models

Organotypic hippocampal cultures

We monitored extracellular field potentials in areas CA1 and CA3 simultaneously in organotypic hippocampal slice

Table 3. Hits discovered with the screen (hits are highlighted in Figs 2F, G).

Drug name	Concentration	Integrated, normalized lactate production	Integrated, normalized LDH production	p_{lactate}	p_{LDH}	SSMD _{lactate}	SSMD _{LDH}
Celecoxib + Phenytoin	10 + 100 $\mu\text{mol/L}$	0.41	0.49	2.133E-07	3.355E-05	-42.04	-11.83
Celecoxib + Phenytoin	10 + 100 $\mu\text{mol/L}$	0.43	0.64	7.663E-07	2.267E-04	-30.52	-7.29
Celecoxib	10 $\mu\text{mol/L}$	0.59	0.70	0.0001	0.0006	-9.60	-5.57
Celecoxib + Phenytoin	10 + 100 $\mu\text{mol/L}$	0.30	0.39	0.0001	1.374E-05	-9.51	-14.81
Celecoxib	10 $\mu\text{mol/L}$	0.72	0.75	0.0001	0.0006	-8.25	-5.60
API-2 (Triciribine)	0.5 $\mu\text{mol/L}$	0.40	0.30	0.0002	0.0007	-7.47	-5.45
Cycloheximide	1 $\mu\text{mol/L}$	0.54	0.34	0.0003	1.879E-08	-6.85	-77.17
TTX	1 $\mu\text{mol/L}$	0.53	0.61	0.0004	0.0008	-6.17	-5.27
Taurine	100 $\mu\text{mol/L}$	0.73	0.32	0.0005	3.627E-05	-5.97	-11.60
Celecoxib	10 $\mu\text{mol/L}$	0.69	0.58	0.0006	0.0008	-5.62	-5.34
LDN-212320 (10-10)	3 $\mu\text{mol/L}$	0.57	0.76	0.0007	0.0002	-5.54	-7.55
Akt 1/2 kinase inhibitor	1 $\mu\text{mol/L}$	0.75	0.54	0.0007	0.0055	-5.42	-3.15
Akt 1/2 kinase inhibitor	0.5 $\mu\text{mol/L}$	0.85	0.59	0.0008	0.0002	-5.33	-7.39
Phenytoin	100 $\mu\text{mol/L}$	0.48	0.57	4.460E-05	0.0001	-5.23	-4.34
Doxepin	10 $\mu\text{mol/L}$	0.62	0.80	0.0011	0.0050	-4.90	-3.22
Rapamycin (DIV3-28)	20 nmol/L	0.59	0.14	0.0011	0.0034	-4.84	-3.60
TTX	1 $\mu\text{mol/L}$	0.48	0.60	0.0013	0.0060	-4.66	-3.07
Celecoxib	10 $\mu\text{mol/L}$	0.58	0.59	0.0014	0.0001	-4.56	-9.66
API-2 (Triciribine)	0.2 $\mu\text{mol/L}$	0.70	0.49	0.0031	0.0024	-3.70	-3.96
Topiramate	100 $\mu\text{mol/L}$	0.82	0.79	0.0036	0.0423	-3.53	-1.70
Kynurenic acid	3 mmol/L	0.51	0.65	0.0004	0.0050	-3.51	-2.16
TTX + Fluoxetine	1 + 1 $\mu\text{mol/L}$	0.63	0.55	0.0049	0.0004	-3.24	-6.32
Phenobarbital + Bumetanide	100 + 10 $\mu\text{mol/L}$	0.86	0.81	0.0052	0.0420	-3.20	-1.70
TTX	1 $\mu\text{mol/L}$	0.58	0.76	0.0058	0.0114	-3.10	-2.56
TTX	1 $\mu\text{mol/L}$	0.53	0.52	0.0059	0.0370	-3.09	-1.78
Rapamycin (DIV 3-14)	20 nmol/L	0.67	0.41	0.0088	0.0010	-2.76	-4.92
Vinblastine	0.01 $\mu\text{mol/L}$	0.66	0.55	0.0096	0.0031	-2.69	-3.70
Neuregulin-1	10 ng/mL	0.80	0.76	0.0096	0.0010	-2.69	-5.02
LDN-72457 (5-1)	10 $\mu\text{mol/L}$	0.70	0.75	0.0103	0.0049	-2.64	-3.25
Picropodophyllotoxin	0.5 $\mu\text{mol/L}$	0.71	0.28	0.0110	0.0038	-2.59	-3.50
Rapamycin (DIV3-14)	20 nmol/L	0.59	0.12	0.0135	0.0032	-2.44	-3.67
Acetylcysteine	50 $\mu\text{mol/L}$	0.85	0.64	0.0135	0.0038	-2.43	-3.49
Furosemide	1 mmol/L	0.71	0.53	0.0143	0.0038	-2.40	-3.49
Neuregulin-1	100 ng/mL	0.81	0.76	0.0167	0.0013	-2.28	-4.61
Phenytoin	100 $\mu\text{mol/L}$	0.46	0.50	0.0044	0.0033	-2.22	-2.35
Celecoxib	10 $\mu\text{mol/L}$	0.67	0.57	0.0213	0.0023	-2.12	-3.98
Colchicine	0.01 $\mu\text{mol/L}$	0.81	0.48	0.0268	0.0051	-1.97	-3.22
Akt 1/2 kinase inhibitor	1 $\mu\text{mol/L}$	0.79	0.29	0.0315	0.0001	-1.87	-9.43
GCEE	1 mmol/L	0.73	0.47	0.0325	2.938E-05	-1.85	-12.23
Neuregulin-1	1 ng/mL	0.88	0.83	0.0334	0.0018	-1.84	-4.29
Rapamycin (DIV 3 >)	20 nmol/L	0.76	0.46	0.0339	0.0028	-1.83	-3.80
Diazepam + CLP257	1 + 100 $\mu\text{mol/L}$	0.69	0.35	0.0386	0.0002	-1.75	-7.11
Carbamazepine	50 $\mu\text{mol/L}$	0.84	0.56	0.0415	0.0002	-1.71	-7.56
Kynurenic acid	3 mmol/L	0.54	0.60	0.0151	0.0165	-1.68	-1.65

Compounds are organized based on increasing lactate SSMD. P values were calculated relative to vehicle-treated controls from the same pup. Repeated drug-concentration pairs represent replicated experiments in different animals.

cultures at two time points, early (DIV 10–15) and late (DIV 25–20). Extracellular field potentials were recorded with celecoxib, vehicle, or neither. The acute effect of celecoxib was observed 10–20 min after the start of continuous application (Fig. 4C). Celecoxib-treated slices

were compared to vehicle-treated slices to control for any temporal variance in epileptiform activity. In early slice cultures, 10 $\mu\text{mol/L}$ celecoxib significantly reduced frequency of seizure-like activity and the power of the field potential ($n = 8$, $P = 0.01$ and 0.047 for frequency and

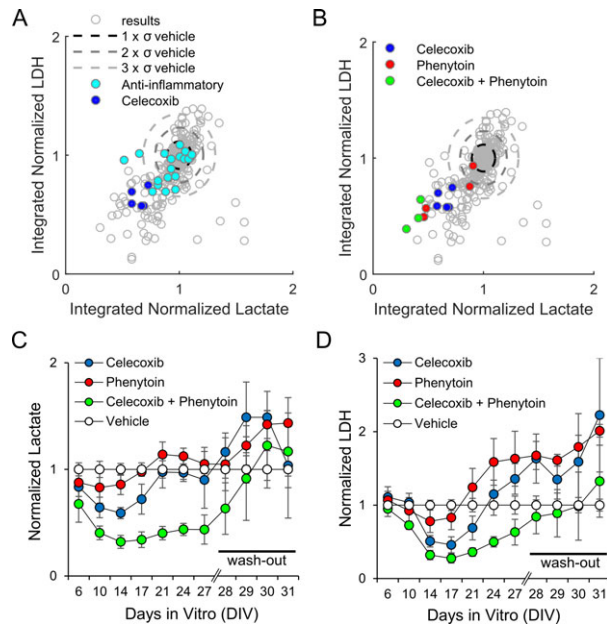


Figure 3. Anticonvulsive and neuroprotective effects of celecoxib, phenytoin, and celecoxib plus phenytoin. (A) The effects of celecoxib ($n = 5$ screens; three slices per screen) and 13 other screened antiinflammatory drugs ($n = 18$ screens; three slices per screen) in comparison with all screened nontoxic compounds. (B) The effects of celecoxib ($10 \mu\text{mol/L}$; $n = 5$ screens), phenytoin ($100 \mu\text{mol/L}$; $n = 4$ screens), and a combination of celecoxib ($10 \mu\text{mol/L}$) plus phenytoin ($100 \mu\text{mol/L}$) ($n = 3$ screens) in comparison with all screened nontoxic compounds. $n = 3$ slices per screen. (C, D) Lactate production (C) and lactate dehydrogenase (LDH) release (D), normalized to controls, for celecoxib ($10 \mu\text{mol/L}$), phenytoin ($100 \mu\text{mol/L}$), and celecoxib ($10 \mu\text{mol/L}$) plus phenytoin ($100 \mu\text{mol/L}$), two separate experiments with three slices per experiment per compound including control ($n = 6$), throughout a 4-week chronic application phase followed by a 4-day wash-out phase.

power reductions, respectively) (Fig. 4D). Celecoxib ($10 \mu\text{mol/L}$) also reduced seizure frequency, total duration of seizures, and total power when compared to baseline activity (prior to celecoxib in the same preparation; $n = 8$, $P = 0.17$, 0.02 , 0.001 , respectively). These data indicate that celecoxib exerts an acute anticonvulsant effect in chronically epileptic brain tissue in vitro (Fig. 4E), and that the inhibition of lactate production by celecoxib (Fig. 3) is due to an effect of celecoxib on seizures.

We also tested celecoxib effects on epileptiform activity recorded extracellularly in older slices with more advanced epilepsy^{30,40} at 25–30 days of culture (Fig. 4F and G). Differences in seizure frequency and power between celecoxib and vehicle-treated groups were significant ($n = 6$ – 8 , $P = 0.003$ and 0.01 , respectively). Frequency and total duration of seizure-like activity decreased with celecoxib treatment ($P = 0.08$ and 0.01 ,

respectively). This indicates an age-independent effect of celecoxib treatment.

Next, we tested the effects of long-term application of celecoxib followed by wash-out to differentiate antiepileptogenic versus reversible anticonvulsant effects of celecoxib. Slices were incubated with $10 \mu\text{mol/L}$ celecoxib for 4 weeks and were then transferred to the recording chamber. Extracellular field potentials were recorded while applying $10 \mu\text{mol/L}$ celecoxib for 2 h to establish the baseline, and then aCSF only for 7 h to wash celecoxib out (Fig. 4H). Seizure-like activity was not observed in most of slices during celecoxib application but reappeared after wash-out (Fig. 4I) ($n = 7$, $P = 0.05$, comparison of seizure frequency in celecoxib and after wash-out). This observation suggests that celecoxib functions as an anticonvulsant rather than an antiepileptogenic drug in organotypic hippocampal culture model of epilepsy.

Rats with kainate-induced epilepsy

Rats were continuously monitored with traditional wired EEG beginning 2 months after epileptogenic kainate administration. Rats were treated with either drug-containing food or food without the drug on day 1 and then observed through day 3.^{32,38} On day 4, the rats were crossed over to the other treatment (i.e., placebo if the first treatment was celecoxib), and observed through day 6. Continuous electrographic recordings through the entire 6-day cycle were analyzed for seizures (Fig. 5B).

Celecoxib treatment caused a significant reduction in seizure frequency compared to placebo (Fig. 5C and D; $P = 0.0116$, paired t-test). Of note, seizures were clustered in this crossover study (Fig. 5B), so that the seizure intervals did not follow a random (Poisson) distribution. To exclude the possibility of a spuriously significant effect of celecoxib due to clustering, we randomly assigned the same clustered distribution of seizure intervals to test how often a significant result could be obtained by chance. Consistent with the paired samples t-test, we found that only two randomizations out of 1000 produced a significant difference with $P \leq 0.0116$ by chance (Fig. 5E). Thus, the in vivo testing in the kainate model of chronic epilepsy supported the findings of the biochemical and electrophysiological in vitro screening.

Discussion

Existing anticonvulsant drugs are ineffective in approximately 30% of patients. This may be due to an anticonvulsant drug discovery pipeline that relies on chemically or electrically induced seizures in otherwise normal brain tissue.^{4,6} However, chronically epileptic tissue is significantly different from normal tissue,⁴¹ and may respond

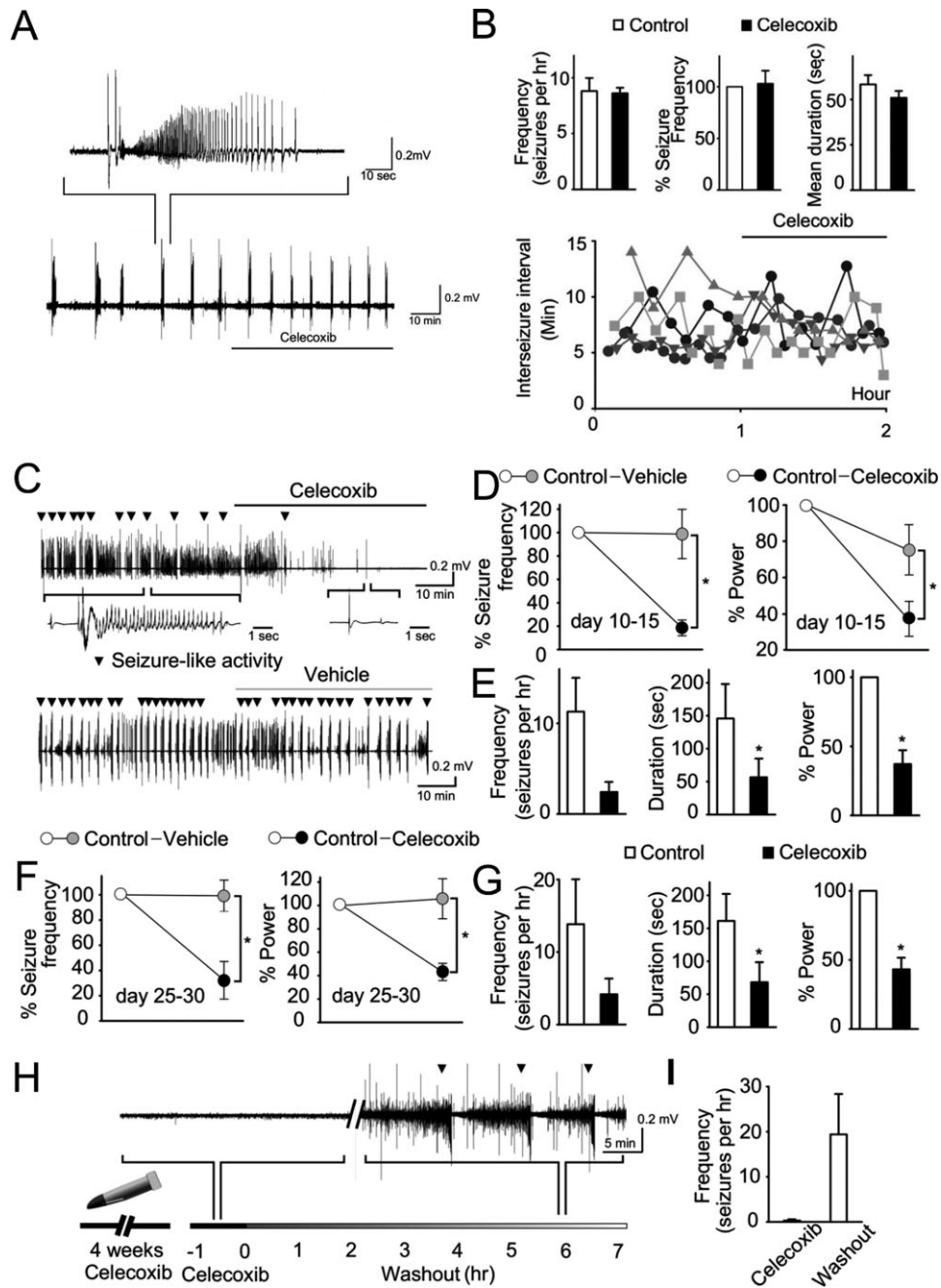


Figure 4. Celecoxib effects in vitro. (A) Application of celecoxib to intact hippocampal preparation in low-Mg aCSF. A representative trace of field potential from intact hippocampal preparation treated with 10 $\mu\text{mol/L}$ celecoxib with induced seizure-like activity is shown. (B) Quantification of frequency and mean duration of seizure-like activity showed that application of celecoxib did not alter those parameters in the intact hippocampal preparation. Different symbols and shading represent results from individual hippocampi. (C) Representative traces of field potential from organotypic hippocampal cultures treated with 10 $\mu\text{mol/L}$ celecoxib or vehicle (DMSO). Inverted triangle indicates seizure-like activity. (D, F) Frequency of seizure and power during bath application of celecoxib (black circle) or vehicle (gray circle) in younger slices (D) day in vitro (DIV 10–15; $n = 8$ slices per group) and older slices (F) (DIV 20–25; $n = 8$ for celecoxib and $n = 6$ for vehicle). (E, G) Comparison of frequency, total duration of seizure, and power, before and during exposure of celecoxib in younger slices (E) and older slices (G). (H, I) Hippocampal slices ($n = 7$) were cultured in the presence of 10 $\mu\text{mol/L}$ celecoxib for 4 weeks and then washed out by artificial CSF for 7 h. Representative recording demonstrates the reappearance of seizure-like activity after wash-out. Error bars represent SEM, $*P < 0.05$ (t-test). Statistical values were determined by one-way analysis of variance or paired t-test.

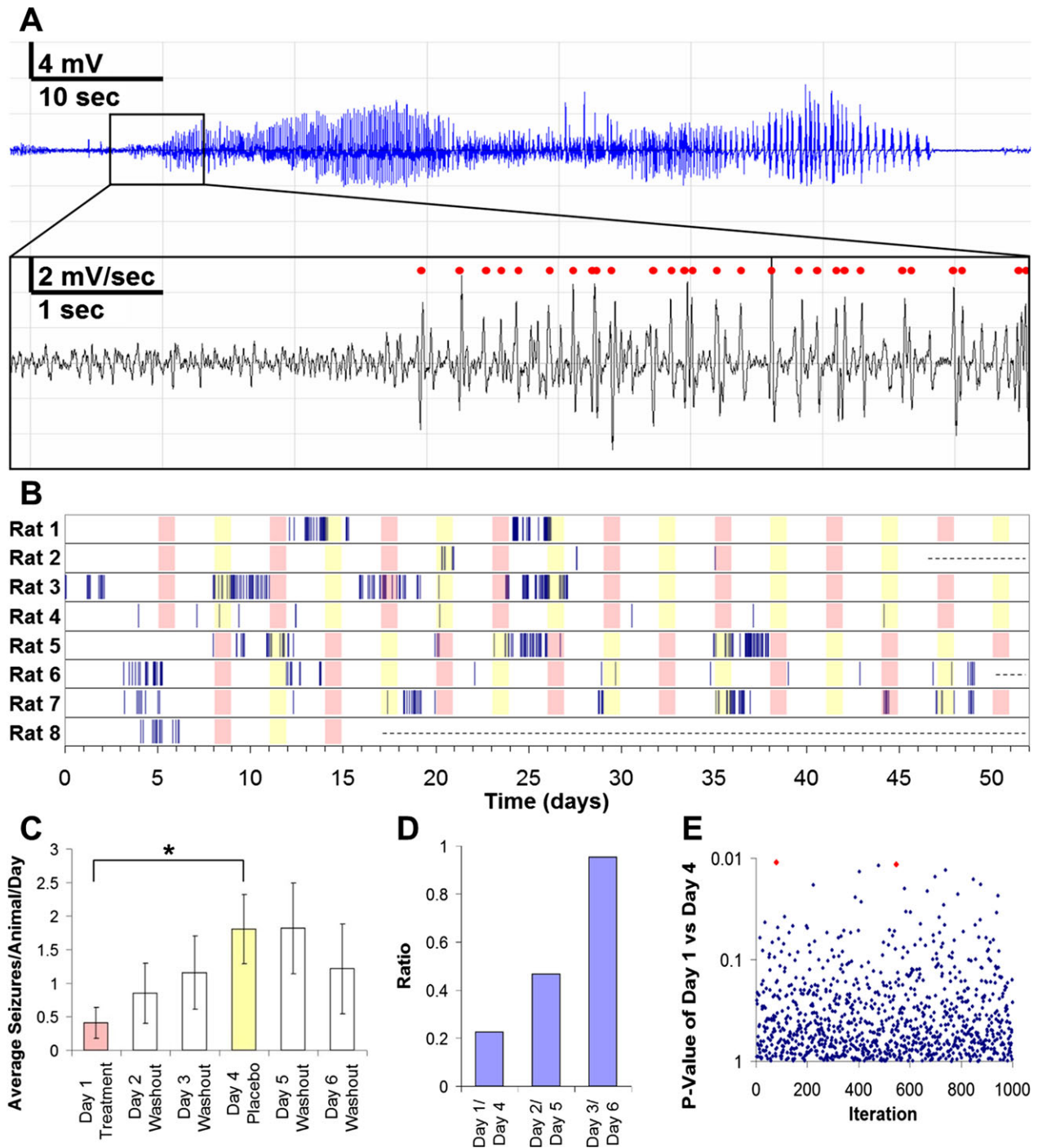


Figure 5. Celecoxib effects in vivo. (A) Raw electroencephalogram (EEG) recording of a seizure (top). First derivative of EEG recording (bottom); spikes marked automatically by dClamp illustrated with red dots. (B) Raster plot of seizure activity in rats ($n = 8$). Celecoxib treatment illustrated in pink; placebo treatment illustrated in yellow; rats removed from experiment illustrated with dashed line. (C) Average number of seizures per rat per day decreases following celecoxib treatment and increases following placebo treatment; data expressed as mean \pm SEM (paired samples t-test, $*P = 0.0116$). (D) Ratio of average number of seizures per rat per day showing effect of celecoxib treatment compared to placebo treatment. (E) Randomization of the order of interseizure intervals for each rat over total time course of experiment demonstrated two cases of false significance ($P \leq 0.0116$, marked in red) for 1000 iterations.

differently to drugs. We developed a three-stage pipeline for discovering new anticonvulsants that relies on chronic epilepsy models at each stage. The organotypic hippocampal culture *in vitro* model of epilepsy was used in the first stage along with biomarkers of seizures to achieve the highest experimental throughput. Electrographic screening in organotypic hippocampal cultures was then used in the second stage to verify biomarker results. Upon electrographic confirmation *in vitro*, *in vivo* experiments were conducted in the kainate model of chronic epilepsy with continuous electrographic monitoring.

The use of organotypic hippocampal cultures, where epileptogenesis occurs on a compressed time scale,^{23,24} and where seizures and seizure-induced cell death can be easily quantified with biomarker assays,^{30,31} allowed us to circumvent the throughput limitations of *in vivo* chronic epilepsy models.⁴ Thus, we were able to screen 140 compounds and combinations of compounds, in over 400 separate drug-concentration experiments, and identify over 40 hits.

We discovered that celecoxib, a selective COX2 inhibitor, was surprisingly effective at inhibiting biomarkers of seizures and seizure-related cell death. We verified these results in a second stage of screening using electrographic seizure quantification in organotypic cultures, and in the final stage of screening *in vivo* in the kainate model. Interestingly, celecoxib was not effective in attenuating acutely induced seizures in the intact hippocampal preparation, demonstrating that an anticonvulsant discovery pipeline that relies on induced seizures in normal brain tissue would likely miss the anticonvulsant effects of this compound.

Several other compounds with similar COX2 inhibitory efficacy exhibited much more modest anticonvulsant effects in the organotypic model (Fig. 3A). Celecoxib also enhances the inhibitory potassium M current and reduces excitatory L-type calcium currents in muscle cells.⁴² However, neither retigabine nor verapamil applied separately had significant activity in this model, suggesting that either these effects are synergistic or that other mechanisms underlie the anticonvulsant effects of celecoxib. Furthermore, the unique efficacy of celecoxib in chronic epilepsy is not readily explained by these particular off-target effects, because compounds with similar agonist/antagonist profiles are also effective in acute models of epilepsy,^{43,44} whereas celecoxib was not (Fig. 4B). Other non-COX2 targets of celecoxib that have been identified in nonneuronal models⁴⁵ may be relevant to its efficacy in chronic epilepsy. An interesting possible mechanism is suggested by the finding that the effects of COX2 antagonists can be substrate-specific,^{46,47} although a celecoxib-specific substrate has not yet been discovered.

Celecoxib has previously been tested in several epilepsy models with quite mixed results.^{48–52} The lack of efficacy

of other COX2 inhibitors has further dampened enthusiasm for this anticonvulsant strategy.⁵³ However, our data clarify that celecoxib is only efficacious in chronic epilepsy models, and a review of the prior mixed results also demonstrates that it is effective in *in vivo* chronic epilepsy models,^{48–50} but not acutely evoked seizures.^{48,51,52} We suggest that this may be a signature of a compound that would be effective for the one-third of epilepsy patients who do not respond to currently available anticonvulsants, all of which were discovered by screening against acutely evoked seizures.

Identification of drugs that prevent or modify epileptogenesis and the progression of epilepsy is an important goal in epilepsy research.^{2,54} The investigation of drug effects on epileptogenesis is relatively straightforward in the first stage of our pipeline. However, there are important caveats. Most anticonvulsants had modest effects (<1.65 standard deviations) on biomarkers of seizure activity and cell death in the *in vitro* screen (Fig. 2F). Phenytoin had the most robust effects of the tested anticonvulsants, but resistance eventually developed (Fig. 3C and previous results³⁰), as occurs after human brain injury.⁵⁵ Thus, many drugs with robust anticonvulsant but not antiepileptogenic effects would be missed in this screen. This suggests that the current screen is an adjunct to, not a replacement of, current anticonvulsant screening methods. The second caveat is that while the lead compound celecoxib inhibited epilepsy for as long as the duration of the experiment without development of resistance (Figs. 3C and 5), this effect washed out immediately when drug was removed (Fig. 4H and I). Thus, the *in vitro* data indicate that this drug is not antiepileptogenic (i.e., it does not prevent the development of epilepsy). Rather the *in vitro* data indicate that it is an anticonvulsant that is effective in conditions where other anticonvulsants fail; that is, during the development of epilepsy after brain trauma.⁵⁶

The only discrepancy between the three stages of evaluation regards the apparent antiepileptogenic effect of celecoxib. Chronic, continuous application of 10 $\mu\text{mol/L}$ celecoxib *in vitro* provided no evidence of an antiepileptogenic effect upon wash-out (Fig. 4H). However, a potential antiepileptogenic effect was observed *in vivo* following single doses administered PO at 6-day intervals (Fig. 5B). Whether this is an effect of dosing interval or *in vivo* metabolism to an antiepileptogenic metabolite will require additional testing.

In the first-stage *in vitro* screening, the compressed time course of epileptogenesis and ease of monitoring biochemical biomarkers of seizures during drug application and wash-out allowed us to determine that celecoxib has an anticonvulsant (but not antiepileptogenic effect) in this model in <5 weeks. In contrast, antiepileptogenic screening in animal models of chronic epilepsy can take

several months.^{57,58} The second stage of screening was also accomplished in a matter of weeks. The final, *in vivo* stage of screening was by far the most labor-intensive, requiring at least 2 months to develop chronic epilepsy with an adequate seizure rate after kainate treatment,⁹ 2 months to execute the crossover trial, and several months to analyze the electrographic data with blind procedures. The speed of the first stage can be further enhanced by parallelization, so that this staged analysis could also be applied to medicinal chemistry optimization of lead compounds.

Acknowledgments

This work was supported by NINDS grants NS072258, NS086364, and NS077908.

Author Contributions

Y.B., Y.S., K-I.P., F.E.D, and K.J.S. designed experiments, analyzed data, and wrote the paper. Y.B., Y.S., K-I.P., B.R., and W.P. conducted experiments. K.L. and W.S. analyzed data. All authors reviewed the manuscript.

Conflicts of Interest

Nothing to report.

References

1. Staley K. Molecular mechanisms of epilepsy. *Nat Neurosci* 2015;18:367–372.
2. Löscher W, Schmidt D. Modern antiepileptic drug development has failed to deliver: ways out of the current dilemma. *Epilepsia* 2011;52:657–678.
3. French JA, White HS, Klitgaard H, et al. Development of new treatment approaches for epilepsy: unmet needs and opportunities. *Epilepsia* 2013;54(Suppl 4):3–12.
4. Wilcox KS, Dixon-Salazar T, Sills GJ, et al. Issues related to development of new antiseizure treatments. *Epilepsia* 2013;54(Suppl 4):24–34.
5. Sabolek HR, Swiercz WB, Lillis KP, et al. A candidate mechanism underlying the variance of interictal spike propagation. *J Neurosci* 2012;32:3009–3021.
6. Galanopoulou AS, Kokaia M, Loeb JA, et al. Epilepsy therapy development: technical and methodologic issues in studies with animal models. *Epilepsia* 2013;54(Suppl 4):13–23.
7. Holmes GL. What is more harmful, seizures or epileptic EEG abnormalities? Is there any clinical data? *Epileptic Disord* 2014;16(Suppl 1):12–22.
8. Gotman J. Relationships between interictal spiking and seizures: human and experimental evidence. *Can J Neurol Sci* 1991;18(4 Suppl):573–576.
9. Williams PA, White AM, Clark S, et al. Development of spontaneous recurrent seizures after kainate-induced status epilepticus. *J Neurosci* 2009;29:2103–2112.
10. Hellier JL, Patrylo PR, Buckmaster PS, Dudek FE. Recurrent spontaneous motor seizures after repeated low-dose systemic treatment with kainate: assessment of a rat model of temporal lobe epilepsy. *Epilepsy Res* 1998;31:73–84.
11. Kadam SD, White AM, Staley KJ, Dudek FE. Continuous electroencephalographic monitoring with radio-telemetry in a rat model of perinatal hypoxia-ischemia reveals progressive post-stroke epilepsy. *J Neurosci* 2010;30:404–415.
12. Gähwiler BH, Capogna M, Debanne D, et al. Organotypic slice cultures: a technique has come of age. *Trends Neurosci* 1997;20:471–477.[cited 2012 Jul 10]
13. De Simoni A, Griesinger CB, Edwards FA. Development of rat CA1 neurones in acute versus organotypic slices: role of experience in synaptic morphology and activity. *J Physiol* 2003;550(Pt 1):135–147.[cited 2012 Jul 10]
14. Prince DA, Parada I, Graber K. Traumatic Brain Injury and Posttraumatic Epilepsy [Internet]. In Noebels JL, Avoli M, Rogawski MA, et al., editors. *Jasper's Basic Mechanisms of the Epilepsies*. Bethesda (MD): National Center for Biotechnology Information (US); 2012 [cited 2016 Jan 26] Available at: <http://www.ncbi.nlm.nih.gov/books/NBK98142/>.
15. Sakaguchi T, Okada M, Kawasaki K. Sprouting of CA3 pyramidal neurons to the dentate gyrus in rat hippocampal organotypic cultures. *Neurosci Res* 1994;20:157–164.
16. Gutiérrez R, Heinemann U. Synaptic reorganization in explanted cultures of rat hippocampus. *Brain Res* 1999;815:304–316.
17. MacVicar BA, Dudek FE. Local synaptic circuits in rat hippocampus: interactions between pyramidal cells. *Brain Res* 1980;184:220–223.
18. Pavlidis P, Madison DV. Synaptic transmission in pair recordings from CA3 pyramidal cells in organotypic culture. *J Neurophysiol* 1999;81:2787–2797.
19. Bausch SB, McNamara JO. Synaptic connections from multiple subfields contribute to granule cell hyperexcitability in hippocampal slice cultures. *J Neurophysiol* 2000;84:2918–2932.[cited 2012 Jul 10].
20. McBain CJ, Boden P, Hill RG. Rat hippocampal slices “*in vitro*” display spontaneous epileptiform activity following long-term organotypic culture. *J Neurosci Methods* 1989;27:35–49.[cited 2012 Jul 10].
21. Gutnick MJ, Wolfson B, Baldino F. Synchronized neuronal activities in neocortical explant cultures. *Exp Brain Res* 1989;76:131–140.
22. Heinemann U, Staley KJ. What is the clinical relevance of *in vitro* epileptiform activity? *Adv Exp Med Biol* 2014;813:25–41.
23. Dyhrfeld-Johnsen J, Berdichevsky Y, Swiercz W, et al. Interictal spikes precede ictal discharges in an organotypic

- hippocampal slice culture model of epileptogenesis. *J Clin Neurophysiol* 2010;27:418–424.
24. Lillis KP, Wang Z, Mail M, et al. Evolution of Network Synchronization during Early Epileptogenesis Parallels Synaptic Circuit Alterations. *J Neurosci* 2015;35:9920–9934.
 25. During MJ, Fried I, Leone P, et al. Direct measurement of extracellular lactate in the human hippocampus during spontaneous seizures. *J Neurochem* 1994;62:2356–2361.
 26. Castillo M, Smith JK, Kwock L. Proton MR spectroscopy in patients with acute temporal lobe seizures. *AJNR Am J Neuroradiol* 2001;22:152–157.
 27. Bonfoco E, Krainc D, Ankarcrona M, et al. Apoptosis and necrosis: two distinct events induced, respectively, by mild and intense insults with N-methyl-D-aspartate or nitric oxide/superoxide in cortical cell cultures. *Proc Natl Acad Sci USA* 1995;92:7162–7166.[cited 2012 Mar 26].
 28. Decker T, Lohmann-Matthes ML. A quick and simple method for the quantitation of lactate dehydrogenase release in measurements of cellular cytotoxicity and tumor necrosis factor (TNF) activity. *J Immunol Methods* 1988;115:61–69.
 29. Korzeniewski C, Callewaert DM. An enzyme-release assay for natural cytotoxicity. *J Immunol Methods* 1983;64:313–320.
 30. Berdichevsky Y, Dzhala V, Mail M, Staley KJ. Interictal spikes, seizures and ictal cell death are not necessary for post-traumatic epileptogenesis in vitro. *Neurobiol Dis* 2012;45:774–785.[cited 2012 Mar 11]
 31. Berdichevsky Y, Dryer AM, Saponjian Y, et al. PI3K-Akt signaling activates mTOR-mediated epileptogenesis in organotypic hippocampal culture model of post-traumatic epilepsy. *J Neurosci* 2013;33:9056–9067.
 32. Ali A, Dua Y, Constance JE, et al. A once-per-day, drug-in-food protocol for prolonged administration of antiepileptic drugs in animal models. *Epilepsia* 2012;53:199–206.
 33. White AM, Williams PA, Ferraro DJ, et al. Efficient unsupervised algorithms for the detection of seizures in continuous EEG recordings from rats after brain injury. *J Neurosci Methods* 2006;152:255–266.
 34. Nakagawa S, Cuthill IC. Effect size, confidence interval and statistical significance: a practical guide for biologists. *Biol Rev Camb Philos Soc* 2007;82:591–605.
 35. Zhang XD. Illustration of SSMD, z score, SSMD*, z* score, and t statistic for hit selection in RNAi high-throughput screens. *J Biomol Screen* 2011;16:775–785.
 36. Dzhala VI, Brumback AC, Staley KJ. Bumetanide enhances phenobarbital efficacy in a neonatal seizure model. *Ann Neurol* 2008;63:222–235.
 37. Hellier JL, Dudek FE. Chemoconvulsant Model of Chronic Spontaneous Seizures. *Current Protocols in Neuroscience*. 31:9.19:9.19.1–9.19.12.
 38. Grabenstatter HL, Clark S, Dudek FE. Anticonvulsant effects of carbamazepine on spontaneous seizures in rats with kainate-induced epilepsy: comparison of intraperitoneal injections with drug-in-food protocols. *Epilepsia* 2007;48:2287–2295.
 39. Tegeder I, Niederberger E, Vetter G, et al. Effects of selective COX-1 and -2 inhibition on formalin-evoked nociceptive behaviour and prostaglandin E(2) release in the spinal cord. *J Neurochem* 2001;79:777–786.
 40. Dzhala V, Staley KJ. Acute and chronic efficacy of bumetanide in an in vitro model of posttraumatic epileptogenesis. *CNS Neurosci Ther* 2015;21:173–180.
 41. Miyata H, Hori T, Vinters HV. Surgical pathology of epilepsy-associated non-neoplastic cerebral lesions: a brief introduction with special reference to hippocampal sclerosis and focal cortical dysplasia. *Neuropathology* 2013;33:442–458.
 42. Brueggemann LI, Mackie AR, Mani BK, et al. Differential effects of selective cyclooxygenase-2 inhibitors on vascular smooth muscle ion channels may account for differences in cardiovascular risk profiles. *Mol Pharmacol* 2009;76:1053–1061.
 43. Hadar EJ, Yang Y, Sayin U, Rutecki PA. Suppression of pilocarpine-induced ictal oscillations in the hippocampal slice. *Epilepsy Res* 2002;49:61–71.
 44. Qiu C, Johnson BN, Tallent MK. K⁺ M-current regulates the transition to seizures in immature and adult hippocampus. *Epilepsia* 2007;48:2047–2058.
 45. Schönthal AH. Direct non-cyclooxygenase-2 targets of celecoxib and their potential relevance for cancer therapy. *Br J Cancer* 2007;97:1465–1468.
 46. Hermanson DJ, Hartley ND, Gamble-George J, et al. Substrate-selective COX-2 inhibition decreases anxiety via endocannabinoid activation. *Nat Neurosci* 2013;16:1291–1298.
 47. Hermanson DJ, Gamble-George JC, Marnett LJ, Patel S. Substrate-selective COX-2 inhibition as a novel strategy for therapeutic endocannabinoid augmentation. *Trends Pharmacol Sci* 2014;35:358–367.
 48. Gobbo OL, O'Mara SM. Post-treatment, but not pre-treatment, with the selective cyclooxygenase-2 inhibitor celecoxib markedly enhances functional recovery from kainic acid-induced neurodegeneration. *Neuroscience* 2004;125:317–327.
 49. Jung K-H, Chu K, Lee S-T, et al. Cyclooxygenase-2 inhibitor, celecoxib, inhibits the altered hippocampal neurogenesis with attenuation of spontaneous recurrent seizures following pilocarpine-induced status epilepticus. *Neurobiol Dis* 2006;23:237–246.
 50. Schlichtiger J, Pekcec A, Bartmann H, et al. Celecoxib treatment restores pharmacosensitivity in a rat model of pharmacoresistant epilepsy. *Br J Pharmacol* 2010;160:1062–1071.
 51. Baik EJ, Kim EJ, Lee SH, Moon C. Cyclooxygenase-2 selective inhibitors aggravate kainic acid induced seizure

- and neuronal cell death in the hippocampus. *Brain Res* 1999;843:118–129.
52. Fischborn SV, Soerensen J, Potschka H. Targeting the prostaglandin E2 EP1 receptor and cyclooxygenase-2 in the amygdala kindling model in mice. *Epilepsy Res* 2010;91:57–65.
53. Rojas A, Jiang J, Ganesh T, et al. Cyclooxygenase-2 in epilepsy. *Epilepsia* 2014;55:17–25.
54. Kovács R, Heinemann U. Models in research of pharmacoresistant epilepsy: present and future in development of antiepileptic drugs. *Curr Med Chem* 2014;21:689–703.
55. Temkin NR, Dikmen SS, Wilensky AJ, et al. A randomized, double-blind study of phenytoin for the prevention of post-traumatic seizures. *N Engl J Med* 1990;323:497–502.
56. Temkin NR. Preventing and treating posttraumatic seizures: the human experience. *Epilepsia* 2009;50(Suppl 2):10–13.
57. Pitkänen A, Nehlig A, Brooks-Kayal AR, et al. Issues related to development of antiepileptogenic therapies. *Epilepsia* 2013;54(Suppl 4):35–43.
58. Pitkänen A, Lukasiuk K, Dudek FE, Staley KJ. Epileptogenesis. *Cold Spring Harb Perspect Med* 2015;5(10): a022822.

Supporting Information

Additional Supporting Information may be found online in the supporting information tab for this article:

Figure S1. Lactate and LDH in cultures after different concentrations of celecoxib were applied starting from DIV 3. Results are presented in cumulative form (DIV 6, DIV 6 + 11, DIV 6 + 11 + 14, etc.). Note toxicity of 100 $\mu\text{mol/L}$ celecoxib indicated by higher LDH release on DIV 6 (3 days after celecoxib application). Each point is an average of results from $n = 3$ cultures.

Table S1. Results of the screen, organized in alphabetical order. Each drug-concentration pair has been applied to three slice cultures, and compared to three vehicle-treated slice cultures. Duplicate drug-concentration pairs represent repeated experiments.